

COSMOS: A Hybrid Adaptive Optimizer for Memory-Efficient Training of LLMs*

Liming Liu¹ Zhenghao Xu¹ Zixuan Zhang¹ Hao Kang¹
 Zichong Li¹ Chen Liang² Weizhu Chen² Tuo Zhao¹

Abstract

Large Language Models (LLMs) have demonstrated remarkable success across various domains, yet their optimization remains a significant challenge due to the complex and high-dimensional loss landscapes they inhabit. While adaptive optimizers such as AdamW are widely used, they suffer from critical limitations, including an inability to capture interdependencies between coordinates and high memory consumption. Subsequent research, exemplified by SOAP, attempts to better capture coordinate interdependence but incurs greater memory overhead, limiting scalability for massive LLMs. An alternative approach aims to reduce memory consumption through low-dimensional projection, but this leads to substantial approximation errors, resulting in less effective optimization (e.g., in terms of per-token efficiency). In this paper, we propose COSMOS, a novel hybrid optimizer that leverages the varying importance of eigensubspaces in the gradient matrix to achieve memory efficiency without compromising optimization performance. The design of COSMOS is motivated by our empirical insights and practical considerations. Specifically, COSMOS applies SOAP to the leading eigensubspace, which captures the primary optimization dynamics, and MUON to the remaining eigensubspace, which is less critical but computationally expensive to handle with SOAP. This hybrid strategy significantly reduces memory consumption while maintaining robust optimization performance, making it particularly suitable for massive LLMs. Numerical experiments on various datasets and transformer architectures are provided to demonstrate the effectiveness of COSMOS. Our code is available at <https://github.com/lliu606/COSMOS>.

1 Introduction

The optimization of Large Language Models (LLMs) is fundamental to their success, enabling these models to achieve state-of-the-art performance across diverse tasks. However, the high-dimensional and non-convex loss landscapes inherent to LLMs, which can contain hundreds of billions or even trillions of parameters (Brown et al., 2020; Achiam et al., 2023), present significant optimization challenges. Adaptive optimizers, such as Adam (Kingma, 2014) and its variants AdamW (Loshchilov, 2017), have emerged as de facto standards due to their ability to dynamically adjust learning rates based on the second moment of the gradient matrix. Despite their

*¹ Georgia Tech, ²Microsoft. Correspondence to lliu606, zhenghaoxu, zhang3105, tourzhao@gatech.edu

widespread adoption, these methods suffer from two critical limitations that impede their effectiveness and scalability in the context of increasingly large and complex LLMs:

- One limitation of Adam and its variants lies in its coordinate-wise use of adaptive learning rates. While this approach dynamically adjusts learning rates for individual parameters based on their gradient history, it inherently fails to capture interdependencies between coordinates. By treating each parameter independently, this method essentially implements an efficient diagonal approximation of the preconditioning matrix. Although this reduces computational complexity, it inadequately represents the intricate curvature information of the loss landscape, particularly in the high-dimensional spaces characteristic of LLMs. Consequently, this approach often leads to suboptimal parameter updates, especially in scenarios where parameter interactions are significant, such as in the complex architectures of large language models (Zhang et al., 2024a).
- Another limitation of Adam and its variants lies in the substantial memory requirement for storing per-parameter adaptive learning rates and gradient statistics. As LLM sizes increase, it becomes prohibitively large, impeding scalability.

To address the limitations of Adam and its variants, researchers have pursued two main approaches. The first approach, exemplified by algorithms such as Shampoo (Gupta et al., 2018) and the more recent SOAP (Vyas et al., 2024), employs sophisticated techniques to capture curvature information and parameter interdependencies. These methods utilize rotational matrices, derived through (approximate) singular value decomposition (SVD) of the gradient matrix, to provide a more comprehensive representation of the loss landscape’s geometry. This approach allows for a better approximation of the full preconditioning matrix, enabling the capture of inter-coordinate dependencies. However, the improved capability of representing parameter interactions comes at the cost of substantial computational and memory overhead (approximately twice of memory usage of Adam for transformers), rendering these algorithms challenging to implement for large-scale LLMs, where memory efficiency is crucial.

The second approach focuses on reducing memory consumption through various approximation techniques. Algorithms such as AdaFactor (Shazeer and Stern, 2018) and Adam-mini (Zhang et al., 2024b) aim to decrease memory usage by approximating the second moment of the gradient matrix. Adam-mini employs a component-specific approach, averaging second moments neuron-wise for certain layers (e.g., output embeddings, value projections, and MLP layers) and head-wise for others (e.g., query and key projections). Meanwhile, AdaFactor utilizes a rank-1 approximation of the second moments. While these methods effectively reduce memory consumption, their approximations often oversimplify the complex structure of the gradient matrix’s moments, leading to a significant loss of critical curvature information and potentially compromising optimization performance. The trade-off between memory efficiency and the preservation of essential gradient statistics remains a crucial challenge in the development of scalable optimizers for LLMs.

More recent approaches, such as GaLore (Zhao et al., 2024a) and MUON (Jordan et al., 2024), have attempted to strike a balance between computational complexity, memory consumption, and optimization performance in LLM training. GaLore, which can be viewed as a memory-efficient

variant of SOAP, approximates the first and second moments of the gradient matrix in the leading eigensubspace. While this approach effectively reduces memory consumption, [Liang et al. \(2024\)](#) find that its effectiveness diminishes for sequence lengths exceeding 256. MUON, essentially an approximation of Shampoo based on some Newton-Schulz transformation proposed in [Bernstein and Newhouse \(2024\)](#), aims to decrease computational complexity. However, this algorithm tends to overfit to the eigensubspaces of the gradient matrix at the current iteration, failing to account for their dynamic nature throughout the optimization process. These methods, while innovative, highlight the ongoing challenge of developing optimizers that are both scalable and effective for LLMs.

In this paper, we propose COSMOS, a novel hybrid optimizer that addresses the limitations of existing methods by exploiting the varying importance of eigensubspaces in the gradient matrix. Our approach decomposes the gradient into two parts: a projection onto the leading eigensubspace and a projection onto the remaining eigensubspace. The leading eigensubspace captures the most significant directions of change in the gradient, typically corresponding to the most important optimization dynamics. For this part, we apply a SOAP-like optimization strategy, tailored specifically to this reduced-dimensional space. The remaining eigensubspace, while less critical, still significantly influences optimization performance.

To address this, we employ MUON as a more efficient alternative to SOAP for this high-dimensional space. Such a hybrid approach allows COSMOS to maintain optimization effectiveness while significantly reducing memory requirements, potentially enabling the training of even larger LLMs or the use of increased batch sizes. Central to our method are (1) the exponential moving averages (EMAs) of the gradient matrix’s first and second moments, which provide smoothed estimates of recent gradient statistics, enhancing the stability of parameter updates and (2) an efficient one-step power update to identify the top k eigenvectors (where k is usually small, only 5%–10% of the original dimension) that capture these crucial gradient directions, designating them as the leading eigensubspace. The design of COSMOS is motivated by empirical insights and practical considerations gleaned from extensive experimentation with large language models, offering a promising solution for scaling up LLM training.

We highlight the key contributions of this paper as follows:

- We propose a novel hybrid optimization strategy. This leads us to develop the COSMOS algorithm, which synergizes the strengths of SOAP and MUON by decomposing the gradient matrix into eigensubspaces of varying importance.
- COSMOS achieves significant memory consumption reduction compared to the SOAP algorithm, while achieving equally or better optimization performance.
- Unlike GaLore, COSMOS’s performance does not degrade when the sequence length exceeds 256.

The rest of the paper is organized as follows: Section 2 reviews the related work; Section 3 presents the COMOS algorithm; Section 4 presents our extensive numerical experiments; Section 5 draws a brief conclusion.

2 Related Work

The optimization of LLMs has seen significant advancements in recent years, with various approaches aimed at improving efficiency and performance. This section discusses key related works in adaptive optimization, memory-efficient techniques, and specialized algorithms for LLMs.

Coordinate-wise Adaptive Optimizers: Adam (Kingma, 2014) and its variant AdamW (Loshchilov, 2017) have become de facto standards in deep learning optimization due to their ability to dynamically adjust learning rates based on the first and second moments of the gradients. However, these methods treat parameters independently, failing to capture interdependencies between coordinates. This limitation can lead to suboptimal updates, especially in the complex architectures of LLMs. Other adaptive optimizers such as Lion (Chen et al., 2023), Sophia (Liu et al., 2023), and Adafactor (Shazeer and Stern, 2018; Zhai et al., 2022) have shown comparable performance to AdamW in LLM pretraining but have not significantly surpassed it, suggesting the need for non-diagonal preconditioners.

Second-Order Optimizers: Researchers have explored second-order optimization techniques for training large models. These methods can be broadly categorized into Hessian-free approaches and Hessian estimation methods. Hessian-free methods, such as those proposed by Martens (2010) and Martens and Grosse (2015), optimize without explicitly computing the Hessian matrix. On the other hand, Hessian estimation methods maintain an efficient approximation of the Hessian for neural networks. Notable examples include KFAC (Martens and Grosse, 2015) and Shampoo (Gupta et al., 2018).

- **KFAC and Its Variants:** KFAC (Martens and Grosse, 2015) was one of the first approaches to go beyond diagonal preconditioners in neural networks, demonstrating that a layer-wise Kronecker-factored preconditioner approximates the layer-wise Hessian in multi-layer perceptrons (MLPs). Subsequent works (Martens et al., 2018; Osawa et al., 2018) extended KFAC to other architectures. Recent research (George et al., 2018; Gao et al., 2021) has further improved trace and diagonal estimates for KFAC. Efforts to scale up KFAC (Ba et al., 2017; Puiu, 2022b,a; Eschenhagen et al., 2023) have focused on making the inversion step more efficient or enhancing distributed implementations.
- **Shampoo and Its Variants:** Shampoo (Gupta et al., 2018), another second-order optimization algorithm, is motivated by the online learning algorithm Adagrad (Duchi et al., 2011). Shampoo also employs a layer-wise Kronecker-factored preconditioner. A recent distributed implementation of Shampoo (Shi et al., 2023) won an optimization efficiency benchmark (Dahl et al., 2023), highlighting the practical utility of second-order methods in deep learning. Other works (Anil et al., 2020; Peirson et al., 2022; Lin et al., 2024; Wang et al., 2024; Zhao et al., 2024b) have proposed various strategies to improve Shampoo’s scalability.
- **SOAP:** The Shampoo with Adam in the Preconditioner’s eigenbasis (SOAP) algorithm (Vyas et al., 2024) establishes a formal connection between Shampoo and Adafactor. SOAP is equivalent to running Adafactor in the eigenbasis of Shampoo’s preconditioner, leading to a simpler and computationally efficient algorithm. By continually updating the running aver-

age of the second moment in the current (slowly changing) coordinate basis, SOAP mitigates the performance degradation associated with less frequent eigendecomposition computations. SOAP has shown significant improvements over AdamW in per-token efficiency.

Memory-Efficient Optimizers: As LLM sizes increase, memory efficiency becomes crucial. Several approaches have been proposed to reduce the memory footprint of optimizers:

- **Adam-mini:** [Zhang et al. \(2024b\)](#) achieve comparable performance than AdamW with a 50% smaller memory footprint. It reduces memory by carefully partitioning parameters into blocks and assigning a single learning rate to each block based on the Hessian structure of neural networks.
- **Adafactor:** [Shazeer and Stern \(2018\)](#) use a low-rank approximation of the second moments to reduce memory consumption. It has been widely used in transformer-based models due to its memory efficiency.
- **GaLore:** [Zhao et al. \(2024a\)](#) reduce Adam’s memory footprint by maintaining momentum in a low-rank subspace derived from the singular value decomposition (SVD) of the gradients. However, its effectiveness diminishes for sequence lengths exceeding 256, as shown in [Liang et al. \(2024\)](#).
- **MUON:** The MUON optimizer ([Jordan et al., 2024](#)) can be viewed as an efficient approximation of Shampoo. It employs a Newton-Schulz transformation to approximately implement the Kronecker-factored preconditioner. While computationally more complex than Adam, MUON only adds minor overhead to the overall training time due to efficient parallelization of matrix operations.

These advancements in optimization techniques highlight the ongoing efforts to improve the training efficiency and performance of LLMs. However, each approach comes with its own trade-offs in terms of computational complexity, memory requirements, and optimization performance. Our work builds upon these insights to develop a hybrid approach that aims to balance these factors effectively, combining the strengths of different methods to achieve both memory efficiency and robust optimization performance for massive LLMs.

3 COSMOS: A Hybrid Adaptive Optimizer

We present a novel hybrid optimizer – COSMOS, which can achieve memory efficiency without compromising optimization performance for training LLMs. Without loss of generality, we use m and n to denote the numbers of rows and columns in a m by n matrix, and we assume $m > n$. For simplicity, we use the following notations.

- **Matrix Sign Operator ([Roberts, 1980](#)):** Given a matrix $X \in \mathbb{R}^{m \times n}$, we consider its SVD decomposition $X = UDV^\top$, where $D \in \mathbb{R}^{n \times n}$ is a diagonal matrix containing all singular values of X , and $U \in \mathbb{R}^{m \times m}$ and $V \in \mathbb{R}^{n \times n}$ are left and right singular vector matrices, respectively. We define

$$\text{MatSgn}(X) = UV^\top.$$

The Shampoo algorithm uses the matrix sign operator to normalize the first moment of the stochastic gradient.

- Newton Schulz (NS) transformation: Given a matrix $X_0 \in \mathbb{R}^{m \times n}$, where $\|X_0\|_F \leq 1$, we define

$$\text{NS5}(X_0) = X_5.$$

where X_5 is obtained by

$$X_{k+1} = aX_k + bX_k X_k^\top X_k + cX_k X_k^\top X_k X_k^\top X_k$$

for $k = 0, 1, \dots, 4$ with $a = 3.4445$, $b = -4.7750$ and $c = 2.0315$. The NS transformation was mentioned in [Bernstein and Newhouse \(2024\)](#) to approximate the matrix sign operator without specifying the coefficient. [Jordan et al. \(2024\)](#) later used an ad-hoc gradient based approach to find such a set of coefficients.

- Normalization operator:

$$\text{NORM}(X) = \sqrt{n}X/\|X\|_F, \quad (1)$$

where $\|\cdot\|_F$ denotes the Frobenius norm. The normalization operator is used to normalize the output of the NS transformation.

- Gram–Schmidt procedure: $\text{QR}(X)$.
- Compute the top- r eigenvectors: $\text{SVD}(X, r)$.

We summarize COSMOS in Algorithm 1.

Algorithm 1 COSMOS for an $m \times n$ layer W . Per layer, we maintain four matrices: $U \in \mathbb{R}^{n \times r}$, $S \in \mathbb{R}^{r \times r}$, $V \in \mathbb{R}^{m \times r}$ and $M \in \mathbb{R}^{m \times n}$.

input Learning rate η , combination weight γ , projection rank $r \ll n$, momentum parameters (β_1, β_2) , perturbation parameter ϵ . For simplicity, we omit the initialization.

- 1: **for** $t = 0, \dots$ **do**
- 2: Sample batch \mathcal{M}_t
- 3: $G_t \leftarrow \nabla_W \phi_{\mathcal{M}_t}(W_t)$
- 4: $M_t \leftarrow \beta_1 M_{t-1} + (1 - \beta_1)G_t$
- 5: $U_t \leftarrow \text{QR}(\beta_2 U_{t-1} S_{t-1} + (1 - \beta_2)G_t^\top G_t U_{t-1})$
- 6: $S_t \leftarrow U_t^\top (\beta_2 U_{t-1} S_{t-1} U_{t-1}^\top + (1 - \beta_2)G_t^\top G_t) U_t$
- 7: $V_t \leftarrow \beta_2 V_{t-1} + (1 - \beta_2)(G_t U_t) \odot (G_t U_t)$
- 8: $A_t = \begin{pmatrix} M_t U_t / (1 - \beta_1^t) \\ \sqrt{(V_t + \epsilon) / (1 - \beta_2^t)} \end{pmatrix} U_t^\top$
- 9: $B_t \leftarrow \text{NORM}\left(\text{NS5}\left(\frac{M_t - M_t U_t U_t^\top}{\|M_t - M_t U_t U_t^\top\|_F}\right)\right)$
- 10: $\tilde{G}_t \leftarrow A_t + \gamma \cdot B_t \cdot \sqrt{m}$
- 11: $W_{t+1} \leftarrow W_t - \eta \cdot \text{NORM}(\tilde{G}_t)$
- 12: **end for**

We have two remarks regarding the differences between COSMOS and SOAP (Algorithm 2¹):

Remark 1. Lines 4–8 in Algorithm 1 can be viewed as a low-rank variant of SOAP with significantly lower memory usage. Specifically, Line 4 obtains the Exponential Moving Average (EMA) of G_t – denoted by M_t . Line 5 approximates the leading eigenbases of M_t – denoted by U_t – by running a simple power iteration on the approximate EMA of $G_t^\top G_t$. Note that we maintain the low dimensional projection of the EMA of $G_t^\top G_t$ – denoted by S_t as in Line 6. When computing the approximate EMA of $G_t^\top G_t$, we can project S_t back to the original space. Line 7 then obtains the EMA of the second moment of the stochastic gradient projected onto the low dimensional eigensubspace of M_t – denoted by V_t . Line 8 first applies an Adam-like adaptive update in the low dimensional eigensubspace of M_t , and then projects the update back to the original space – denoted by A_t .

As can be seen, COSMOS only needs to maintain four matrices in the memory: $M_t \in \mathbb{R}^{m \times n}$, $U_t \in \mathbb{R}^{n \times r}$, $S_t \in \mathbb{R}^{r \times r}$ and $V_t \in \mathbb{R}^{m \times r}$. In sharp contrast, SOAP needs to maintain $M_t \in \mathbb{R}^{m \times n}$, $L_t \in \mathbb{R}^{n \times n}$, $U_t \in \mathbb{R}^{n \times n}$ and $V_t \in \mathbb{R}^{m \times n}$. The resulting memory overhead is which is significantly larger than that of COSMOS.

Remark 2. Line 9 in Algorithm 1 is a MUON-like update – denoted by B_t , but only applied to the complementary subspace of M_t – denoted by $M_t(I - U_t U_t^\top)$. Line 10 obtains a weighted combination of B_t and the SOAP-like update A_t . Line 11 then applies such a combination to update the weight.

The NS transformation does not need to maintain any additional matrix in the memory, and therefore incurs no additional memory overhead.

Algorithm 2 (One-side) SOAP for an $m \times n$ layer W . Per layer, we maintain four matrices: $U_t \in \mathbb{R}^{n \times n}$, $L \in \mathbb{R}^{n \times n}$, $V \in \mathbb{R}^{m \times n}$ and $M \in \mathbb{R}^{m \times n}$.

input Learning rate η , momentum parameters (β_1, β_2) , perturbation parameter ϵ . For simplicity, we omit the initialization.

```

1: for  $t = 0, \dots$  do
2:   Sample batch  $\mathcal{M}_t$ 
3:    $G_t \leftarrow \nabla_W \phi_{\mathcal{M}_t}(W_t)$ 
4:    $M_t \leftarrow \beta_1 M_{t-1} + (1 - \beta_1) G_t$ 
5:    $L_t \leftarrow \beta_2 G_t^\top G_t U_{t-1} + (1 - \beta_2) G_t^\top G_t U_{t-1}$ 
6:    $U_t \leftarrow \text{QR}(L_t U_{t-1})$ 
7:    $G'_t \leftarrow M_t U_t$ 
8:    $V_t \leftarrow \beta_2 V_{t-1} + (1 - \beta_2)(G'_t \odot G'_t)$ 
9:    $A_t = \begin{pmatrix} G'_t / (1 - \beta_1^t) \\ \sqrt{(V_t + \epsilon) / (1 - \beta_2^t)} \end{pmatrix} U_t^\top$ 
10:   $W_{t+1} \leftarrow W_t - \eta A_t$ 
11: end for

```

We next compare COSMOS with MUON (Algorithm 3) and have the following two remarks:

¹To fairly compare with COSMOS, we only consider the one-sided SOAP, which is discussed in Section 7.1 of [Vyas et al. \(2024\)](#).

Remark 3. The NS transformation in MUON behaves like a fixed point iteration without changing the eigensubspace of M_t . Therefore, the resulting preconditioning is dedicated to the eigenbases of M_t . In contrast, COSMOS adopts a power iteration to the approximate EMA of $G_t^\top G_t$ for incrementally updating the projection matrix U_t from U_{t-1} . Therefore, we can separately control the training dynamics of U_t , yielding a smoother transition of eigenbases for preconditioning, which potentially leads to better optimization performance.

Remark 4. We propose a new normalization procedure NORM in (1). It is motivated by the observation that NS5 is only an approximation of the standard Newton Schulz iteration, and the singular values of its output are not exactly 1's, especially for small singular values. Therefore, the Frobenius norm of the output may substantially deviate from the desirable \sqrt{n} (corresponding to the case where all singular values equal to 1). In contrast, our normalization procedure guarantees the Frobenius norm of the output to be exactly \sqrt{n} , which improves training stability.

Algorithm 3 MUON for an $m \times n$ layer W . Per layer, we maintain one matrix: $M \in \mathbb{R}^{m \times n}$.

input Learning rate η , momentum parameters β_1 . For simplicity, we omit the initialization.

- 1: **for** $t = 0, \dots$ **do**
- 2: Sample batch \mathcal{M}_t
- 3: $G_t \leftarrow \nabla_W \phi_{\mathcal{M}_t}(W_t)$
- 4: $M_t \leftarrow \beta_1 M_{t-1} + (1 - \beta_1) G_t$
- 5: $B_t \leftarrow \text{NS5}(M_t / \|M_t\|_F)$
- 6: $W_{t+1} \leftarrow W_t - \eta B_t \cdot \sqrt{m}$
- 7: **end for**

Memory Usage Comparison: For comparison, we list the memory usage of the optimization states in Adam, Adam-mini, SOAP, MUON and COSMOS for training transformer models in Table 1. For simplicity, we assume that the attention weight matrices $W_Q, W_K, W_V, W_O \in \mathbb{R}^{d \times d}$ and the MLP weight matrices $W_1 \in \mathbb{R}^{d \times 4d}$ and $W_2 \in \mathbb{R}^{4d \times d}$. Note that in practical LLMs, the dimensionalities of W_1 and W_2 might slightly vary. Moreover, we assume that the rank of the projection is $r = 0.05d$ for COSMOS.

We remark that Table 1 only compares the optimization states. In practice, however, besides the optimization states, the overall memory usage also includes the model weights and intermediate variables used in the forward and backward passes as well as additional memory overhead of I/O and computation. Therefore, we present a more detailed and practical memory profiling for training LLaMA-1B model in Section 4.

Table 1: Memory usage of the optimization states in different algorithms for training transformer models.

Adam	Adam-mini	SOAP	MUON	COSMOS
$24d^2$	$12d^2$	$66d^2$	$12d^2$	$13.5d^2$

Two-sided COSMOS. For simplicity, we only consider the one-side version of COSMOS in this paper. Like SOAP, COSMOS can be further generalized to a two-sided version. See more details in Appendix B.

4 Experiments

We evaluate the performance of COSMOS on pre-training various sizes of LLMs, in comparison with baseline algorithms including Adam (Kingma, 2014), Adam-mini (Zhang et al., 2024b), GaLore (Zhao et al., 2024a), SOAP (Vyas et al., 2024) and MUON (Jordan et al., 2024). Note that for SOAP, MUON and COSMOS, the embedding and output weights are trained by Adam.

Models and Datasets. We train LLaMA-type models (Touvron et al., 2023) on the C4 dataset (Raffel et al., 2020), which is a colossal, cleaned version of Common Crawl’s web crawl corpus for pre-training. We conduct comprehensive experiments and ablation studies on 130M models and demonstrate the token efficiency of COSMOS. We then scale up to 350M and 1B models to showcase the memory efficiency and small computational overhead of COSMOS. Due to limited computational resources, experiments on these larger models are less comprehensive, while still capable of illustrating the efficacy of our method. We train for one epoch on a portion of the C4 dataset, ranging from 5B to 26B tokens, and scaling with the model size according to the scaling law (Kaplan et al., 2020). We set the maximum sequence length as 1024 by default. Besides LLaMA models and C4 dataset, we also experiment with GPT-2 (Radford et al., 2019) on WikiText-103 dataset (Merity et al., 2016), presented in Appendix C.2.

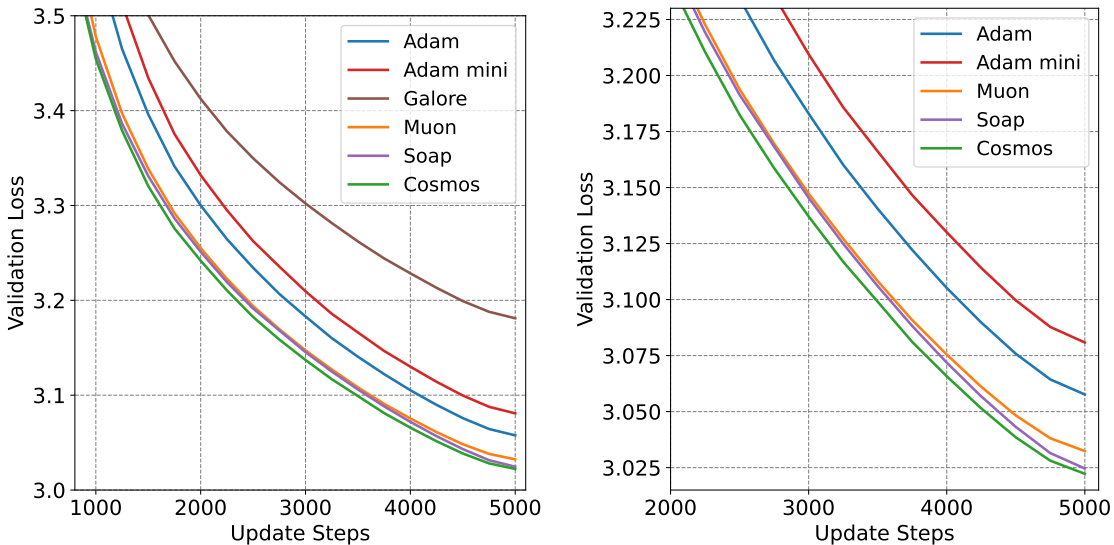


Figure 1: Performance on LLaMA-130M. COSMOS consistently outperforms baseline methods. In the right plot, we hide GaLore to better compare the performance of COSMOS with SOAP and MUON, as the curves are close in the left plot.

4.1 Comparison on LLaMA-130M

For LLaMA-130M, we train on a 5B subset of the C4 dataset. We compare COSMOS’s validation loss with that of Adam, Adam-mini, GaLore, MUON, and SOAP.

Hyperparameters. For each method, we tune the corresponding learning rate to obtain optimal performance. We select the rank $r = 64$ for COSMOS and $r = 256$ for GaLore. To avoid multiple hyperparameter tuning, we set the discount factor in COSMOS as $\gamma = \eta/\eta_0$, where η_0 is the learning rate of Adam for training the embedding and output weights in the implementation of COSMOS. Other hyperparameter choices follow [Zhao et al. \(2024a\)](#) and are provided in detail in Appendix [A.1.1](#).

Main results. We plot the validation loss curves in Figure 1. As illustrated, COSMOS consistently outperforms MUON with better stability and is comparable to SOAP. This showcases that our hybrid approach leveraging the leading eigensubspace captures the most important information for efficient update, allowing COSMOS to achieve similar per-token efficiency as SOAP. In addition, all three methods outperform the vanilla Adam and are much better than Adam-mini and GaLore, validating that inter-coordinate dependence is crucial for efficient optimization. We report the final validation perplexity in Table 2.

Table 2: Validation perplexity after training on C4 dataset. We train for 5000 steps on 130M and 350M models and 13000 steps on 1B model. COSMOS achieves the best validation perplexity.

Size(Tokens)	130M(5B)	350M(10B)	1B(26B)
Adam	21.28	17.28	12.97
Adam-mini	21.78	-	-
GaLore	24.07	19.03	-
SOAP	20.59	16.32	-
MUON	20.69	16.49	12.57
COSMOS	20.54	16.21	12.46

Ablation on learning rates. We experiment with different learning rates while keeping the rank $r = 64$ and discount factor $\gamma = \eta/\eta_0$ for COSMOS. As shown in the Table 3, COSMOS is not very sensitive to the learning rate, and it achieves the best performance at 5e-4. As a comparison, MUON is more sensitive to the learning rate, and it underperforms COSMOS across all learning rates.

Table 3: Validation perplexity under different learning rates. We set $\gamma = \eta/\eta_0$ and $r = 64$ for COSMOS. Our method outperforms MUON across all learning rates.

lr	2e-4	5e-4	1e-3	2e-3
MUON	21.72	20.75	20.69	26.74
COSMOS	21.17	20.54	20.62	21.00

Ablation on rank and discount factor. We also experiment with different ranks r and discount

factors γ while keeping the learning rate as $5e-4$ for COSMOS, and the results are summarized in Table 4. As illustrated, COSMOS is not very sensitive to r and γ , and the best discount factor is around 0.25 to 0.5 across different ranks. In practice, our choice $\gamma = \eta/\eta_0$ falls in this range, so it serves as a valid heuristic that prevents extra tuning of γ . We provide details in Appendix A. Moreover, we observe that as rank increases, COSMOS performs slightly worse and is more sensitive to the choice of γ . One possible explanation is that when the rank is large, the top- r eigenvalues of M_t contain some smaller values that are close to the remaining eigenvalues. For these eigenvalues, the one-step power iteration (Line 5 in Algorithm 1) cannot accurately approximate their corresponding eigensubspaces, leading to larger approximation errors and worse performance.

Table 4: Validation perplexity of COSMOS under different ranks r and discount factors γ . Our method is not very sensitive to r and γ , and consistently outperforms MUON (20.69) except for only one configuration ($r = 128, \gamma = 1$).

$r \setminus \gamma$	0.1	0.25	0.5	1
32	20.58	20.55	20.54	20.54
64	20.62	20.54	20.57	20.61
128	20.65	20.58	20.63	20.72

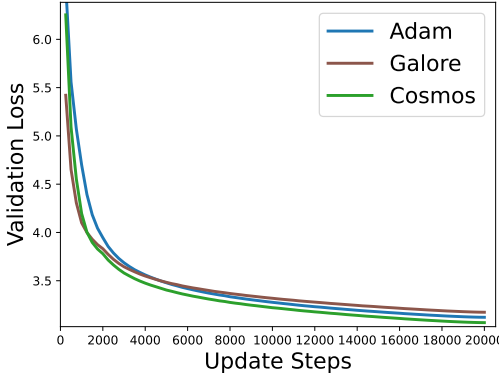


Figure 2: Comparison of COSMOS, Adam, and GaLore on 256 sequence length. The performance of GaLore on shorter sequences does not deteriorate as for long sequences, validating the correctness of our implementation.

Effect of normalization. COSMOS applies a normalization step (Line 9 in Algorithm 1) after the NS transformation. To illustrate that normalization alone cannot fully explain the COSMOS’s efficiency, we apply the same normalization to MUON and compare their performances. As shown in Figure 3, MUON with normalization performs similarly to the version without normalization, and both are worse than COSMOS. This implies that normalization does not contribute as much as other components of COSMOS, including the SOAP-like update in the leading eigensubspace. We present the same experiment with LLaMA-350M in Appendix C.1.

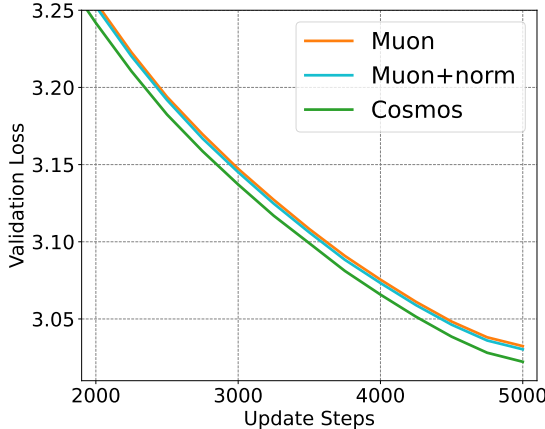


Figure 3: Comparison of COSMOS, MUON and MUON with normalization for LLaMA-130M on C4. MUON’s performance does not differ by much with normalization, implying that normalization is not the dominant reason why COSMOS outperforms MUON.

GaLore degradation on long sequences. In our experiment, we observe that GaLore performs much worse than COSMOS and other baselines including Adam. To validate the correctness of our implementation, we compare GaLore with COSMOS and Adam on 256 sequence length as adopted in [Zhao et al. \(2024a\)](#). As shown in Figure 2, GaLore and Adam are comparable in this shorter sequence setting, suggesting that GaLore degenerates on long sequences. This observation aligns with [Liang et al. \(2024\)](#), while a similar phenomenon appearing in fine-tuning is reported by [Pan et al. \(2024\)](#). In contrast, COSMOS consistently outperforms Adam from short to long sequences without suffering from degradation.

4.2 Scaling up to LLaMA-350M and LLaMA-1B

To further illustrate the efficacy of COSMOS, we scale up to larger models and more tokens. For LLaMA-350M, we train on a 10B subset of the C4 dataset for 5000 steps. We compare COSMOS with Adam, GaLore, MUON, and SOAP. For LLaMA-1B, we train on a 26B subset for 13000 steps. Given limited computation resources, we compare COSMOS with Adam and MUON. Adam serves as the standard baseline, while MUON achieves better performance than Adam while requiring less memory and little computational overhead. Although SOAP demonstrated superior performance among baselines, we exclude it from our comparison as its complete training for the 1B model exceeds our available resources. More experiment details are provided in Appendices [A.1.2](#) and [A.1.3](#).

Main results of token efficiency. Figures 4 and 5 display the validation loss curves for the 350M and 1B models, and Table 2 presents their final validation perplexities. COSMOS demonstrates superior performance compared to all baselines across both model sizes, matching the results on the 130M model and showcasing consistent token efficiency across different model sizes.

Memory and computation time profiling. To illustrate the memory efficiency and small computation overhead of COSMOS, we conduct a profiling experiment on LLaMA-1B to track memory

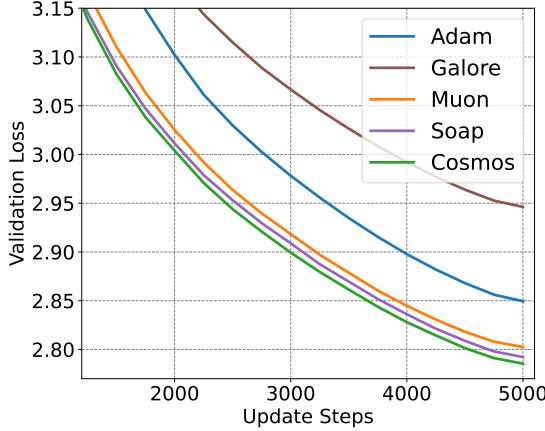


Figure 4: Performance of LLaMA-350M trained on C4 dataset. COSMOS consistently outperforms baseline methods.

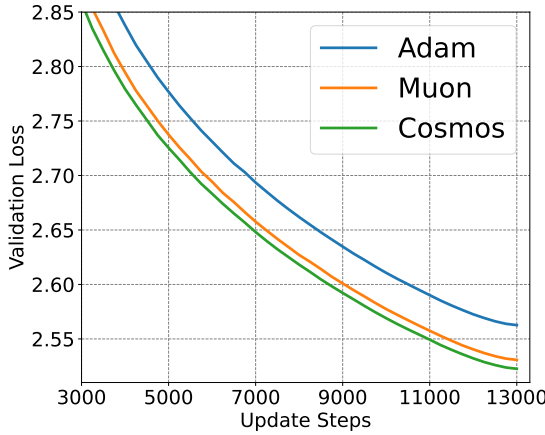


Figure 5: Performance of LLaMA-1B trained on C4 dataset. COSMOS consistently outperforms Adam and MUON.

usage and wall-clock time. We fix the batch size 10 and gradient accumulation step 25 for all methods for a fair comparison. We record the maximum GPU memory usage and time spent during the entire forward-backward propagation and optimizer update process for one iteration. As shown in table 5, COSMOS achieves much lower maximum GPU memory usage than Adam (**6.8%**) and SOAP (**19.4%**), with slightly more overhead compared to MUON. In terms of wall-clock time per iteration, COSMOS is comparable to MUON and is much better than SOAP. The fastest Adam method cannot achieve the same level of token efficiency as COSMOS. Therefore, COSMOS strikes a good balance between token and memory/computation overheads, achieving the best final perplexity at a much lower cost.

Throughput. To better compare the methods in practical setting, we evaluate the maximal batch size and throughput of COSMOS and baselines. We experiment on a single NVIDIA A100 GPU with 80GB memory. The input sequence length is set to 1024. As shown in Table 6, COSMOS is

Table 5: GPU memory usage and wall-clock time per iteration on 1B model. We fix the batch size to be 10 for all methods. COSMOS has significantly less memory usage than SOAP and is comparable to memory-efficient methods like Adam-mini and MUON, without introducing much computation overhead.

Method	Memory	Wall-clock time
Adam	62.75 G	34.73 s
SOAP	72.58 G	39.51 s
MUON	58.25 G	35.56 s
COSMOS	58.47 G	35.75 s

Table 6: System performance on single NVIDIA A100-80G GPU and corresponding throughput (number of samples processed per second on C4 dataset) of 1B model. Max batch size is defined as the maximum number of samples that fit within the GPU’s memory capacity. Throughput is reported as the number of samples the GPU processes per second (samples/s)

Method	Max batch size	Throughput(sample/s)
Adam	13	7.24
SOAP	10	6.33
MUON	14	7.23
COSMOS	14	7.07

10.8% faster than SOAP and comparable to MUON.

4.3 Summary of Numerical Experiments

We summarize our main experiment results. (1) COSMOS achieves the best token efficiency comparable to SOAP. (2) Our memory usage and throughput are significantly better than SOAP. (3) Our method performs consistently across different model sizes, different sequence lengths, and different hyperparameter configurations.

5 Conclusion

We develop a hybrid adaptive optimizer, COSMOS, which leverages the varying importance of eigensubspaces in the gradient matrix to achieve token efficiency, memory efficiency, and high computation throughput simultaneously. By decomposing the gradient matrix into leading and remaining eigensubspaces and applying SOAP-like and MUON-like updates to them correspondingly, COSMOS uses significantly less memory than SOAP while achieving equal or better optimization performance. Comprehensive experiments show that COSMOS performs consistently well across different settings.

References

ACHIAM, J., ADLER, S., AGARWAL, S., AHMAD, L., AKKAYA, I., ALEMAN, F. L., ALMEIDA, D., ALTENSCHMIDT, J., ALTMAN, S., ANADKAT, S. ET AL. (2023). Gpt-4 technical report. *arXiv preprint arXiv:2303.08774*.

ANIL, R., GUPTA, V., KOREN, T., REGAN, K. and SINGER, Y. (2020). Scalable second order optimization for deep learning. *arXiv preprint arXiv:2002.09018*.

BA, J., GROSSE, R. and MARTENS, J. (2017). Distributed second-order optimization using kronecker-factored approximations. In *International Conference on Learning Representations*.

BERNSTEIN, J. and NEWHOUSE, L. (2024). Modular duality in deep learning. *arXiv preprint arXiv:2410.21265*.

BROWN, T., MANN, B., RYDER, N., SUBBIAH, M., KAPLAN, J. D., DHARIWAL, P., NEELAKANTAN, A., SHYAM, P., SASTRY, G., ASKELL, A. ET AL. (2020). Language models are few-shot learners. *Advances in neural information processing systems*, **33** 1877–1901.

CHEN, X., LIANG, C., HUANG, D., REAL, E., WANG, K., LIU, Y., PHAM, H., DONG, X., LUONG, T., HSIEH, C.-J. ET AL. (2023). Symbolic discovery of optimization algorithms. *arXiv e-prints arXiv-2302*.

DAHL, G. E., SCHNEIDER, F., NADO, Z., AGARWAL, N., SASTRY, C. S., HENNIG, P., MEDAPATI, S., ESCHENHAGEN, R., KASIMBEG, P., SUO, D. ET AL. (2023). Benchmarking neural network training algorithms. *arXiv preprint arXiv:2306.07179*.

DUCHI, J., HAZAN, E. and SINGER, Y. (2011). Adaptive subgradient methods for online learning and stochastic optimization. *Journal of machine learning research*, **12**.

ELFWING, S., UCHIBE, E. and DOYA, K. (2018). Sigmoid-weighted linear units for neural network function approximation in reinforcement learning. *Neural networks*, **107** 3–11.

ESCHENHAGEN, R., IMMER, A., TURNER, R. E., SCHNEIDER, F. and HENNIG, P. (2023). Kronecker-factored approximate curvature for modern neural network architectures. *arXiv preprint arXiv:2311.00636*.

GAO, K., LIU, X., HUANG, Z., WANG, M., WANG, Z., XU, D. and YU, F. (2021). A trace-restricted kronecker-factored approximation to natural gradient. In *Proceedings of the AAAI Conference on Artificial Intelligence*, vol. 35.

GEORGE, T., LAURENT, C., BOUTHILLIER, X., BALLAS, N. and VINCENT, P. (2018). Fast approximate natural gradient descent in a kronecker-factored eigenbasis. *arXiv preprint arXiv:1806.03884*.

GUPTA, V., KOREN, T. and SINGER, Y. (2018). Shampoo: Preconditioned stochastic tensor optimization. In *International Conference on Machine Learning*. PMLR.

JORDAN, K., JIN, Y., BOZA, V., JIACHENG, Y., CECISTA, F., NEWHOUSE, L. and BERNSTEIN, J. (2024). Muon: An optimizer for hidden layers in neural networks.
<https://kellerjordan.github.io/posts/muon/>

KAPLAN, J., MCCANDLISH, S., HENIGHAN, T., BROWN, T. B., CHESS, B., CHILD, R., GRAY, S., RADFORD, A., WU, J. and AMODEI, D. (2020). Scaling laws for neural language models. *arXiv preprint arXiv:2001.08361*.

KINGMA, D. P. (2014). Adam: A method for stochastic optimization. *arXiv preprint arXiv:1412.6980*.

LIANG, K., LIU, B., CHEN, L. and LIU, Q. (2024). Memory-efficient llm training with online subspace descent. *arXiv preprint arXiv:2408.12857*.

LIN, W., DANGEL, F., ESCHENHAGEN, R., BAE, J., TURNER, R. E. and MAKHZANI, A. (2024). Can we remove the square-root in adaptive gradient methods? a second-order perspective. *arXiv preprint arXiv:2402.03496*.

LIU, H., LI, Z., HALL, D., LIANG, P. and MA, T. (2023). Sophia: A scalable stochastic second-order optimizer for language model pre-training. *arXiv preprint arXiv:2305.14342*.

LOSHCHILOV, I. (2017). Decoupled weight decay regularization. *arXiv preprint arXiv:1711.05101*.

MARTENS, J. (2010). Deep learning via hessian-free optimization. In *Proceedings of the 27th International Conference on International Conference on Machine Learning*.

MARTENS, J., BA, J. and JOHNSON, M. (2018). Kronecker-factored curvature approximations for recurrent neural networks. In *International Conference on Learning Representations*.

MARTENS, J. and GROSSE, R. (2015). Optimizing neural networks with kronecker-factored approximate curvature. *arXiv preprint arXiv:1503.05671*.

MERITY, S., XIONG, C., BRADBURY, J. and SOCHER, R. (2016). Pointer sentinel mixture models. *arXiv preprint arXiv:1609.07843*.

OSAWA, K., TSUJI, Y., UENO, Y., NARUSE, A., YOKOTA, R. and MATSUOKA, S. (2018). Large-scale distributed second-order optimization using kronecker-factored approximate curvature for deep convolutional neural networks. *arXiv preprint arXiv:1811.12019*.

PAN, R., LIU, X., DIAO, S., PI, R., ZHANG, J., HAN, C. and ZHANG, T. (2024). Lisa: Layerwise importance sampling for memory-efficient large language model fine-tuning. *arXiv preprint arXiv:2403.17919*.

PEIRSON, A., AMID, E., CHEN, Y., FEINBERG, V., WARMUTH, M. K. and ANIL, R. (2022). Fishy: Layerwise fisher approximation for higher-order neural network optimization. In *Has it Trained Yet? NeurIPS 2022 Workshop*.

PUIU, C. O. (2022a). Brand new k-facs: Speeding up k-fac with online decomposition updates. *arXiv preprint arXiv:2210.08494*.

PUIU, C. O. (2022b). Randomized k-facs: Speeding up k-fac with randomized numerical linear algebra. In *International Conference on Intelligent Data Engineering and Automated Learning*.

RADFORD, A., WU, J., CHILD, R., LUAN, D., AMODEI, D., SUTSKEVER, I. ET AL. (2019). Language models are unsupervised multitask learners. *OpenAI blog*, **1** 9.

RAFFEL, C., SHAZER, N., ROBERTS, A., LEE, K., NARANG, S., MATENA, M., ZHOU, Y., LI, W. and LIU, P. J. (2020). Exploring the limits of transfer learning with a unified text-to-text transformer. *Journal of machine learning research*, **21** 1–67.

ROBERTS, J. D. (1980). Linear model reduction and solution of the algebraic riccati equation by use of the sign function. *International Journal of Control*, **32** 677–687.

SHAZEER, N. and STERN, M. (2018). Adafactor: Adaptive learning rates with sublinear memory cost. *arXiv preprint arXiv:1804.04235*.

SHI, H.-J. M., LEE, T.-H., IWASAKI, S., GALLEGOS-POSADA, J., LI, Z., RANGADURAI, K., MUDIGERE, D. and RABBAT, M. (2023). A distributed data-parallel pytorch implementation of the distributed shampoo optimizer for training neural networks at-scale. *arXiv preprint arXiv:2309.06497*.

SU, J., AHMED, M., LU, Y., PAN, S., BO, W. and LIU, Y. (2024). Roformer: Enhanced transformer with rotary position embedding. *Neurocomputing*, **568** 127063.

TOUVRON, H., MARTIN, L., STONE, K., ALBERT, P., ALMAHAI, A., BABAEI, Y., BASHLYKOV, N., BATRA, S., BHARGAVA, P., BHOSALE, S. ET AL. (2023). Llama 2: Open foundation and fine-tuned chat models. *arXiv preprint arXiv:2307.09288*.

VYAS, N., MORWANI, D., ZHAO, R., SHAPIRA, I., BRANDFONBRENER, D., JANSON, L. and KAKADE, S. (2024). Soap: Improving and stabilizing shampoo using adam. *arXiv preprint arXiv:2409.11321*.

WANG, S., ZHOU, P., LI, J. and HUANG, H. (2024). 4-bit shampoo for memory-efficient network training. *arXiv preprint arXiv:2405.18144*.

ZHAI, X., KOLESNIKOV, A., HOULSBY, N. and BEYER, L. (2022). Scaling vision transformers. In *Proceedings of the IEEE/CVF conference on computer vision and pattern recognition*.

ZHANG, Y., CHEN, C., DING, T., LI, Z., SUN, R. and LUO, Z.-Q. (2024a). Why transformers need adam: A hessian perspective. *arXiv preprint arXiv:2402.16788*.

ZHANG, Y., CHEN, C., LI, Z., DING, T., WU, C., YE, Y., LUO, Z.-Q. and SUN, R. (2024b). Adam-mini: Use fewer learning rates to gain more. *arXiv preprint arXiv:2406.16793*.

ZHAO, J., ZHANG, Z., CHEN, B., WANG, Z., ANANDKUMAR, A. and TIAN, Y. (2024a). Galore: Memory-efficient llm training by gradient low-rank projection. *arXiv preprint arXiv:2403.03507*.

ZHAO, R., MORWANI, D., BRANDFONBRENER, D., VYAS, N. and KAKADE, S. (2024b). Deconstructing what makes a good optimizer for language models. *arXiv preprint arXiv:2407.07972*.

A Experiment Details

Many aspects of our setup such as models are the same as in [Zhao et al. \(2024a\)](#). We train language models on C4 tokenized with the T5 tokenizer ([Raffel et al., 2020](#)) and report results in terms of validation loss.

Models. We start from the GaLore Codebase ([Zhao et al., 2024a](#)) and train LLaMA models of three sizes: 130M, 350M, and 1B. The models have widths of 768, 1024, and 2048 and depths of 12, 16, and 24. We use the 130M model to explore various ablations as shown in Section 4.1. The MLP hidden dimension of the 130M model is 4 times the width and the hidden dimension of the 350M and 1B model is $\frac{8}{3}$ times the width. The activation function is SiLU ([Elfwing et al., 2018](#)). The architecture uses RoPE positional encodings ([Su et al., 2024](#)). Attention heads are always dimension 64. For more architecture details please refer to [Zhao et al. \(2024a\)](#). We train in mixed precision with FP32.

Algorithms. We use the standard Pytorch implementation of Adam, and the official GaLore implementation provided by [Zhao et al. \(2024a\)](#). Since Two-Sided SOAP is too memory consuming and is not within our comparison scope, we modify the code provided by [Vyas et al. \(2024\)](#) to apply One-Sided SOAP discussed in [Vyas et al. \(2024\)](#). We use the official Adam-mini implementation provided by [Zhang et al. \(2024b\)](#). For MUON and NS5, we use their implementation provided by [Jordan et al. \(2024\)](#) in their Github records. We implement our COSMOS starting from an older version of Pytorch implementation of AdamW.

Default hyperparameters. In all algorithms, we choose momentum $\beta_1 = 0.9$, $\beta_2 = 0.98$ and smoothing term $\epsilon = 1e-8$ to align with the standard hyperparameter choice of Adam. We use the linear learning rate schedule to decay the learning rate to 0. To align with [Zhao et al. \(2024a\)](#), we set the warmup ratio to be 10% and weight decay to be 0.

Token counts. For all of our runs we use a sequence length of 1024. For the 130M model, we set the batch size to be 960, and for the 350M and 1B models, we set the batch size to be 2000. We train the 130M and 350M models for 5k steps and train the 1B model for 13k steps. Thus the number of training tokens for the 130M mode $\approx 5B$, which is beyond the “chinchilla optimal” number of tokens. The numbers of training tokens for the 350M model and 1B model are 10B and 26B respectively, which follow the chinchilla optimal” number of tokens.

A.1 Learning rate tuning

To avoid unfair comparisons caused by excessive hyperparameter tuning, for all algorithms we set the learning rate as the only tunable hyperparameter in all the main results in Section 4. The rank r for COSMOS for all main results is fixed at 64.

A.1.1 Tuning on 130M model

For Adam, we tune the learning rate on {5e-4, 1e-3, 2e-3, 4e-3, 8e-3}. In our experiments, 2e-3 is the optimal learning rate and 8e-3 diverges. Then for SOAP, we also tune the learning rate on {5e-4, 1e-3, 2e-3, 4e-3}. For Adam-mini, we just use the optimal learning rate of Adam, which is 2e-3.

For GaLore, We follow the setting in [Zhao et al. \(2024a\)](#), set rank=256, and scale factor $\alpha = 0.25$. The projection update frequency is 200 for 20k training steps, thus we decrease it to 50 for our 5k training steps. According to [Zhao et al. \(2024a\)](#), the learning rate should be larger than Adam's.

For the implementation of MUON and COSMOS, the embedding and output layer will use Adam while other parts will use MUON/COSMOS algorithm. To avoid multiple hyperparameter tuning, we fix the learning rate for embedding and output layer to 2e-3 and only tune the learning rate of hidden layers, whose optimizer is MUON/COSMOS. To be more specific, we tune the learning rate of hidden layers on {2e-4, 5e-4, 1e-3, 2e-3}.

For COSMOS, as we mentioned before, to avoid tuning γ , we simply set γ to be the ratio of the learning rate of hidden layers to the learning rate of the embedding layer (which is fixed at 2e-3). We find that this trick can provide a satisfactory result without extra tuning on γ . Please note that we find in many extra experiments that this trick isn't the optimal choice for γ . Tuning γ may output a better result.

A.1.2 Tuning on 350M model

For Adam and SOAP, we tune the learning rate on {5e-4, 1e-3, 2e-3, 4e-3}. For GaLore, we set the rank to be 384, projection update frequency to be 50, and scale factor $\alpha = 0.25$. Then we tune the learning rate of GaLore on {5e-3, 1e-2, 2e-2, 4e-2}.

For the implementation of MUON and COSMOS, we still fix the learning rate for embedding and output layer to be 2e-3 and only tune the learning rate of MUON/COSMOS for hidden layers. For MUON and COSMOS, we tune the learning rate on {2e-4, 5e-4, 1e-3}. Also for COSMOS, we still set γ to be the ratio of the learning rate of hidden layers to the learning rate of the embedding layer (which is fixed at 2e-3).

A.1.3 Tuning on 1B Model

We do not have enough resources to tune hyperparameters carefully on the 1B model. For Adam, we first try learning rate $\eta = 2e-3$, but an extremely large loss spike occurred in the early stage. Then we decrease η to 1e-3 and get the result. For MUON and COSMOS, we still fix the learning rate for embedding and output layer to be 2e-3 and tune their learning rate on {2e-4, 5e-4}. For COSMOS, we still set γ to be the ratio of the learning rate of hidden layers to the learning rate of the embedding layer.

A.2 Ablation of r and γ on 130M model

For the ablation experiments on COSMOS in Section 4.1, we tune discount factor γ and rank r together to show COSMOS isn't very sensitive to hyperparameters. We fix the learning rate for embedding and output layers to be 2e-3, fix the learning rate for COSMOS to be 5e-4, and sweep over the cross product of $r \in \{32, 64, 128\}$ and $\gamma \in \{0.1, 0.25, 0.5, 1\}$. With all these hyperparameters COSMOS outputs comparable results to MUON.

A.3 Ablation of normalization

As mentioned in the normalization paragraph in Section 4.1, to exclude the possibility that the better performance of COSMOS than MUON is simply because the normalization function `NORM`, we modify the normalization method of MUON to be `NORM` and rerun the experiments for 130M and 350M models. We still tune the learning rate of MUON + `NORM` on $\{5\text{e-}3, 1\text{e-}2, 2\text{e-}2, 4\text{e-}2\}$, and present their best performance.

A.4 Profiling experiments

We do the profiling experiments on the 1B model. We set the sequence length to 1024, which aligns with our previous settings. We set batch size 10 and accumulation steps 25. Then we record the maximum GPU memory usage and time usage on this setting by using Pytorch API during the entire forward-backward and optimizer update process.

B Two-sided COSMOS

Similar to two-sided SOAP in [Vyas et al. \(2024\)](#), we provide a two-sided variant of COSMOS in Algorithm 4.

Algorithm 4 Two-sided version of COSMOS for a $m \times n$ layer. Per layer, we maintain six matrices: $U \in \mathbb{R}^{n \times r}$, $O \in \mathbb{R}^{m \times r}$, $S, R \in \mathbb{R}^{r \times r}$, $V \in \mathbb{R}^{m \times r}$ and $M \in \mathbb{R}^{m \times n}$.

input Learning rate η , combination weight γ , projection rank $r \ll n$, momentum parameters (β_1, β_2) , perturbation parameter ϵ . For simplicity, we omit the initialization.

- 1: **for** $t = 0, \dots$ **do**
- 2: Sample batch \mathcal{M}_t
- 3: $G_t \leftarrow \nabla_W \phi_{\mathcal{M}_t}(W_t)$
- 4: $M_t \leftarrow \beta_1 M_{t-1} + (1 - \beta_1) G_t$
- 5: $U_t \leftarrow \text{QR}(\beta_2 U_{t-1} S_{t-1} + (1 - \beta_2) G_t^\top G_t U_{t-1})$
- 6: $O_t \leftarrow \text{QR}(\beta_2 R_{t-1} O_{t-1} + (1 - \beta_2) G_t G_t^\top O_{t-1})$
- 7: $S_t \leftarrow U_t^\top (\beta_2 U_{t-1} S_{t-1} U_{t-1}^\top + (1 - \beta_2) G_t^\top G_t) U_t$
- 8: $R_t \leftarrow O_t^\top (\beta_2 O_{t-1} R_{t-1} O_{t-1}^\top + (1 - \beta_2) G_t G_t^\top) O_t$
- 9: $V_t \leftarrow \beta_2 V_{t-1} + (1 - \beta_2) (O_t^\top G_t U_t) \odot (O_t^\top G_t U_t)$
- 10: $A_t = O_t \begin{pmatrix} O_t^\top M_t U_t / (1 - \beta_1^t) \\ \sqrt{(V_t + \epsilon) / (1 - \beta_2^t)} \end{pmatrix} U_t^\top$
- 11: $B_t \leftarrow \text{NORM} \left(\text{NS5} \left(\frac{M_t - O_t^\top O_t M_t U_t U_t^\top}{\|M_t - O_t^\top O_t M_t U_t U_t^\top\|_F} \right) \right)$
- 12: $\tilde{G}_t \leftarrow A_t + \gamma \cdot B_t \cdot \sqrt{m}$
- 13: $W_{t+1} \leftarrow W_t - \eta \cdot \text{NORM}(\tilde{G}_t)$
- 14: **end for**

C Additional Experiments

This section provides supplementary experiments not presented in the main text.

C.1 Additional Experiments for Normalization Ablation

We conduct additional experiments on LLaMA-350M to further validate that normalization is not the main reason for COSMOS outperforming MUON. As shown in Figure 6, normalization does not make much difference to MUON, while COSMOS consistently outperforms both of them.

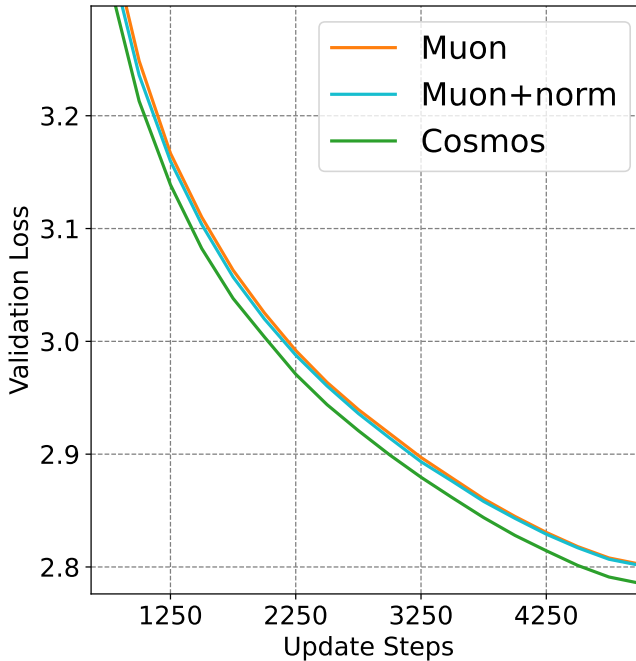


Figure 6: Comparison of COSMOS, MUON and MUON with normalization for LLaMA-350M on C4. MUON’s performance does not differ by much with normalization, implying that normalization is not the dominant reason why COSMOS outperforms MUON.

C.2 Additional Experiments on WikiText

This section provides additional experiments on WikiText (Merity et al., 2016) and GPT-2 (Radford et al., 2019). To be more specific, we train GPT2-small(125M) and GPT2-medium (355M) on the Wikitext-103 dataset. We discard learnable position embeddings and use RoPE (Su et al., 2024) as a replacement. For GPT2-small, we use learning rate 4e-3 for the embedding layer and 4e-4 for MUON/COSMOS. For GPT2-medium, we use learning rate 2e-3 for the embedding layer and 5e-4 for MUON/COSMOS. γ is still set to be the ratio of the hidden layer learning rate to the embedding layer learning rate.

We set the sequence length to be 1024, and the batch size is also 1024. We train both models for 5k steps, which means the models are trained on 5B tokens. For such many training tokens

on Wikitext-103, overfitting will occur and validation loss will start to increase after training for a certain number of steps. Therefore, we use the training loss as the metric for comparison.

The results for GPT2-small and GPT2-medium are provided in Figures 7 and 8, respectively. We observe that COSMOS consistently outperforms MUON, showing that it does not overfit any particular model or dataset.

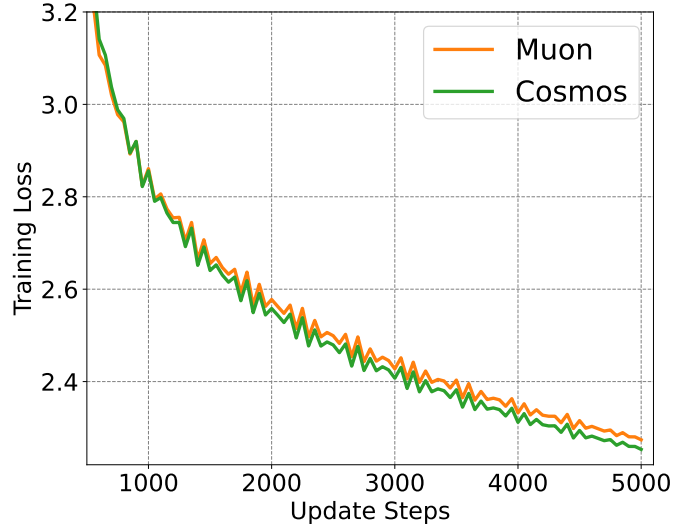


Figure 7: GPT2-small trained on WikiText-103 dataset. COSMOS consistently outperforms MUON.

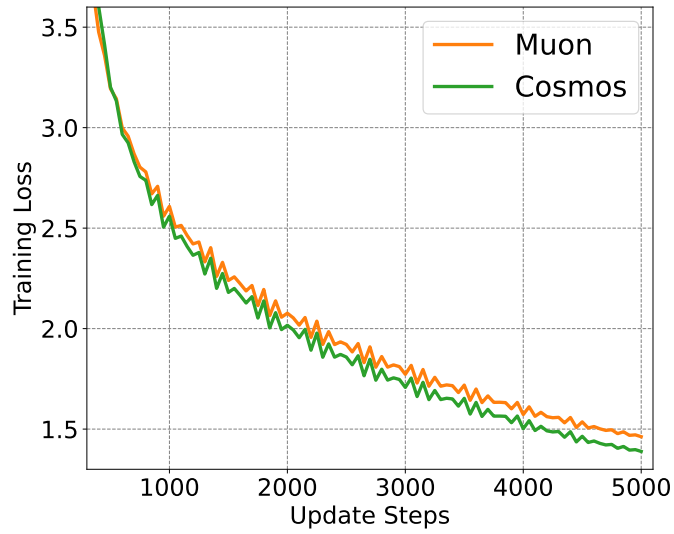


Figure 8: GPT2-medium trained on WikiText-103 dataset. COSMOS consistently outperforms MUON.

C.3 Smaller learning rate for MUON/COSMOS on LLaMA-1B

As discussed in section A.1.3, we tune the learning rate for MUON/COSMOS on $\{2e-4, 5e-4\}$. We find $5e-4$ is better and present its corresponding results in the main text. Here we present the result for $2e-4$ in Figure 9, where COSMOS still outperforms MUON.

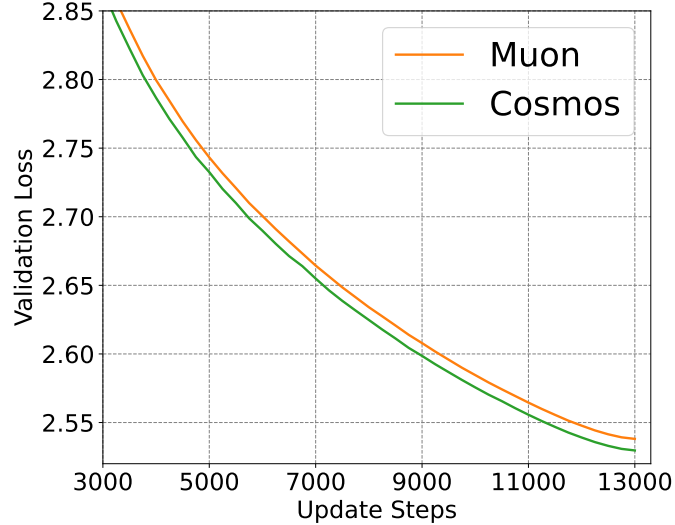


Figure 9: LLaMA-1B trained on C4 dataset with learning rate $2e-4$ for MUON/COSMOS. COSMOS still outperforms MUON.